# Apparatus for X-ray diffraction microscopy and tomography of cryo specimens

T. Beetz [a,b], M.R. Howells [c], C. Jacobsen [a], C.-C. Kao [d], J. Kirz [a,c], E. Lima [a], T.O. Mentes [a,e], H. Miao [a], C. Sanchez-Hanke [d], D. Sayre [a], D. Shapiro [a]

[a] *Department of Physics and Astronomy, Stony Brook University, Stony Brook, NY 11794-3800, USA*
[b] *Center for Functional Nanomaterials, Brookhaven National Laboratory, Upton, NY 11973-5000, USA*
[c] *Advanced Light Source, Lawrence Berkeley National Laboratory, Berkeley, CA 94720, USA*
[d] *National Synchrotron Light Source, Brookhaven National Laboratory, Upton, NY 11973-5000, USA*
[e] *TASC-INFM National Laboratory, 34012 Basovizza (Trieste), Italy*

**Abstract**

An apparatus for diffraction microscopy of biological and materials science specimens is described. In this system, a coherent soft X-ray beam is selected with a pinhole, and the illuminated specimen is followed by an adjustable beamstop and CCD camera to record diffraction data from non-crystalline specimens. In addition, a Fresnel zone plate can be inserted to allow for direct imaging. The system makes use of a cryogenic specimen holder with cryotransfer capabilities to allow frozen hydrated specimens to be loaded. The specimen can be tilted over a range of $\pm 80^\circ$ for three-dimensional imaging; this is done by computer-controlled motors, enabling automated alignment of the specimen through a tilt series. The system is now in use for experiments in soft X-ray diffraction microscopy.

*Key words:* X-ray microscopy, X-ray imaging, X-ray tomography, Diffraction microscopy, Lensless imaging
*PACS:*

## 1. Introduction

Lens-based X-ray microscopy is a well established technique for studying micrometer-sized objects at a present spatial resolution of 20-40 nm. While lenses make direct imaging straighforward, they also can limit the achievable resolution, due both do overall efficiency for radiation-sensitive specimens, and also declining transfer function at high spatial frequencies [1]. In order to obtain the maximum information from the specimen without optics-imposed limits, an alternative approach is to record the continuous diffraction pattern of a non-periodic specimen as first proposed by Sayre [2,3]. This approach has been demonstrated successfully first by Miao *et al.* [4] and more recently by others [5,6], using iterative phasing algorithms [7–9] for the reconstruction of a real-space image.

In previous demonstrations of diffraction microscopy, the sample has been maintained at room temperature and the experiment carried out primarily by the manual adjustment of relevant components. However, it is well known that for biological specimens imaged using ionizing radiation, cryogenic temperatures offer dramatic improvement in the preservation of structural information

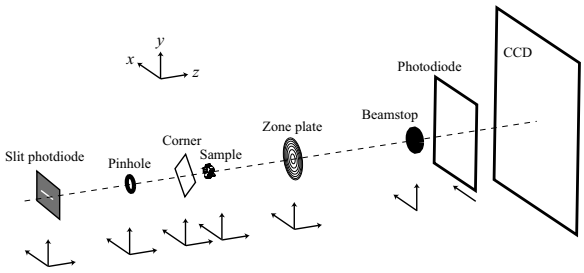


Fig. 1. Schematic of the elements used inside the vacuum chamber. The direction of motion is indicated by arrows. Sample rotation is done around the $x$-axis. Note that only a subset of these elements are in place at any given time.

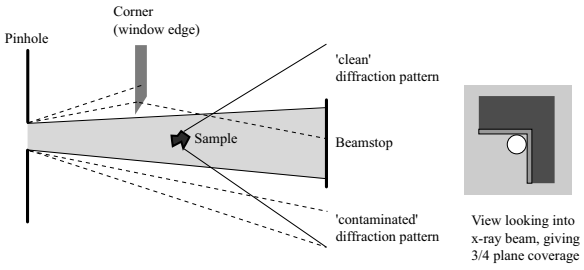


Fig. 2. Illustration of the use of a soft-edged object (in this case the corner of the silicon frame of a broken-out silicon nitride window) to record diffraction data free of the scatter of an upstream coherence-selecting pinhole. The edge of the window frame acts like a prism to refract unwanted scatter away into one quadrant; the opposite corner can then be used in a separate recording to obtain the complete data. This approach was first used in diffraction microscopy experiments by H.N. Chapman, then at Stony Brook.

[10]. Demonstrations of lens-based 3D imaging by means of soft X-ray tomography have been carried out in cryogenic microscopes [11–13]. To obtain a 3D reconstruction of diffraction data, one must rotate the specimen and collect a series of diffraction datasets at different orientations [14]. For these reasons, we have developed a new apparatus with motorized control of its key elements that makes it possible to automate the procedure of collecting such 3D data. The apparatus also has cryotransfer capabilities and the ability to rotate the specimen through an angular range as high as $\pm 80°$. We have therefore been able to develop the methodology for high throughput collection of 3D diffraction data of radiation-sensitive specimens such as biological specimens.

Diffraction microscopy involves a relatively simple setup (Fig. 1). A pinhole is used to select a region of the beam with good spatial coherence and monochromaticity, and the specimen follows closely behind. In many cases, one will follow the pinhole with a silicon window corner used to remove scattering by the pinhole in three quarters of the diffraction plane (Fig. 2). A beamstop is then located in front of a CCD camera which is used to collect the diffraction signal. Diagnostic photodiodes are also located in the chamber, and a zone plate can be inserted for direct imaging of the specimen.

## 2. Specimen illumination

The specimen illumination requirements for diffraction microscopy are different from what most synchrotron beamlines provide. Our goal is to maximize not only the coherent flux, but also the coherent flux density at the location of the specimen by having the total coherent beam size be as close as possible to the oversampling ratio $\sigma$ [15] multiplied by the specimen width $d$. In present practice, this means maximizing the coherent flux within a 20 $\mu$m diameter region. In addition, the monochromaticity requirements are rather modest compared to many other synchrotron experiments [16,17]. As described below, one essentially needs a monochromaticity of half the number of CCD pixels, or $\lambda/(\Delta\lambda) = 700$, at present. Therefore, a beamline that is designed to deliver high energy resolution, with $\lambda/(\Delta\lambda)$ of several thousand, and which places the specimen far from an exit slit where beam has been allowed to diverge to an area of a hundred micrometers or more, is not optimized for diffraction microscopy recordings. For this reason, Howells *et al.* have designed a beamline (beamline 9.0.1 at the Advanced Light Source, Lawrence Berkeley National Laboratory) that uses an off-axis section of a Fresnel zone plate as a monochromator [18]. This beamline makes use of the third harmonic of a 10 cm period undulator. A cylindrical nickel mirror with a radius of 306 m at a grazing incidence

angle of 3° is used to remove most of the undulator X-rays above an energy of about 800 eV. A 0.5 $\mu$m thick, 0.8 mm by 0.8 mm beryllium window removes most of the X-rays produced by the first undulator harmonic. The combination of the nickel mirror and the beryllium window reduces the total power transmitted to the zone plate to 0.1 W at 520 eV and 0.035 W at 750 eV. The monochromator zone plate section consists of 180 nm high gold zones on a 100 nm thick silicon nitride window with an overlying and underlying coating of 100 nm of copper on each side. It is placed directly in the mirror-filtered undulator beam, resulting in a dispersed spectrum below the undulator plane. The zone plate section consists of 2000 half-period zones with an outermost zone width of 250 nm. The area of the zone plate is section is 550 $\mu$m by 550 $\mu$m. Monochromator zone plates have been fabricated both by P. Charalambous of PSC Nanolithography, and by Xradia, Inc. The monochromatic beam is obtained by placing a pinhole at the distance corresponding the focal length of the zone plate. Two monochromator zone plate sections are presently mounted in the beamline: one located 1.16 m upstream of the pinhole for use at 750 eV, and one located 0.78 m upstream of the pinhole for use at 520 eV. For operation at 520 eV, we are presently in the process of equipping the beamline with an order-sorting system consisting of two mirrors with a critical energy of reflection of about 545 eV.

By using as few optics as possible, and by projecting a monochromatic focus onto the pinhole, this beamline delivers a coherent flux of $8 \cdot 10^9$ photons/second into a 4 $\mu$m pinhole, as measured using a XUV photodiode with absolute calibration (International Radiation Detectors). This coherent flux density exceeds that available in previous experiments at beamline X1B (National Synchrotron Light Source, Brookhaven National Laboratory) by about a factor of 200.

## 3. Instrumentation

The experimental chamber features a 4-axis goniometer which accepts standard electron microscopy sample transfer holders to support the specimen (see below for details). This choice was made to conform with well established sample preparation protocols known mainly from electron microscopy. Several optics and beam-defining apertures can be positioned around the sample. The data are recorded on an in-vacuum CCD camera. Fig. 1 shows a schematic of the main elements inside the experimental chamber, along with their directions of motion.

### 3.1. *Goniometer and sample holder*

Sample positioning is done with a motorized four-axis goniometer system provided by JEOL USA, Inc., which is normally a component of their JEM-2010 FasTEM transmission electron microscope. All of the goniometer motor control is outside the vacuum and the sample is inserted into the vacuum chamber via an airlock. Fig. 3 shows the goniometer attached to the vacuum chamber together with a view of the specimen holder emerging from the goniometer assembly inside the vacuum chamber. Custom vacuum fittings were designed to attach the goniometer drives to the experimental chamber.

The main goniometer drive sits horizontally and provides motion in $x$, $y$, $z$, and $\theta$ as described in Fig. 3. When the chamber is aligned so that the axis of the $\theta$ rotation intersects with the X-ray beam, motions of $x$, $y$, and $z$ to place a particlar specimen location in the beam path will then cause that location to remain on axis as the goniometer is rotated. In experiments carried out thus far, the wobble in the specimen position is about 75 $\mu$m over a 90° range in $\theta$, but we are only now implementing methods for fine measurement and correction of the eucentricity of the goniometer system. The motions of these axes are driven by DC motors with encoders.

The sample can be inserted on a sample holder through the goniometer airlock, and the small volume (about 10 ml) can be quickly evacuated. We currently have two standard electron microscopy sample transfer holders that fit the goniometer system. One is a Gatan 630 high-tilt cryo specimen holder (Fig. 4) on which a sample can be main-

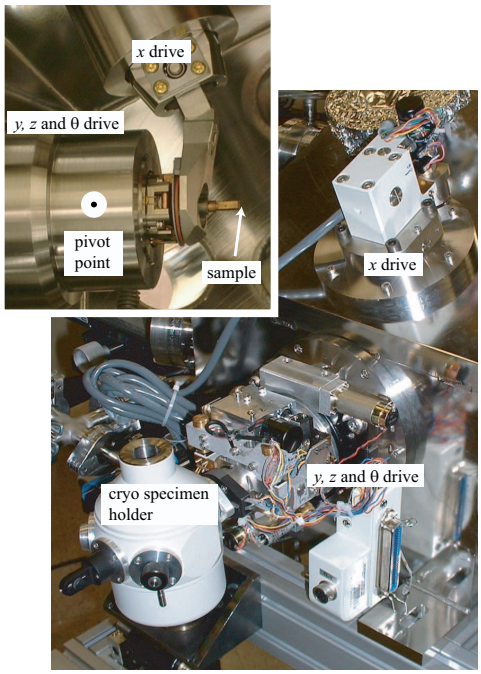


Fig. 3. View of the goniometer system manufactured by JEOL USA, Inc., as incorporated in the diffraction microscope system. Following the coordinate system of Fig. 1, the $\theta$ drive rotates the specimen holder positioning system about a fixed axis. The specimen is then positioned in $y$ and $z$ by motors which move the outside-of-vacuum end of the specimen holder about the pivot point indicated in the inset photo (which was taken from inside the vacuum chamber). Motion in the $x$ direction is provided by an out-of-vacuum motor that pushes against vacuum forces to move the specimen holder within the goniometer sleeve.

tained at about $-178°$ C to minimize radiation damage during data acquisition. The Gatan holder is equipped with almost free-standing slotted copper specimen grids that allow for an angular tilt range of $\pm 80°$. The grids can be retracted between two copper faces, so that cryo specimens are protected from frost during transfer into the chamber vacuum. The second sample holder is a JEOL room temperature holder which can be used for samples that do not require cooling or require non-standard sample mounting.

Fig. 4. View of the Gatan 630 high-tilt cryo sample holder. The dewar can be filled with liquid nitrogen to cool the sample; the specimen region is cooled by thermal conduction through a rod connecting it to this dewar. The small image shows a close-up of the tip of the holder, where a high-tilt copper grid is inserted. The grid can be retracted between two copper plates to protect cryo specimens during transfer into the vacuum chamber, and then extended so that it can be viewed at very high tilt angles (up to about $\pm 80°$).

### 3.2. *Motor stages and drive electronics*

To quickly align various optical components like zone plates, beam defining apertures or phosphor screens, the experimental chamber makes use of two in-vacuum $xyz$ motorized translation stage stacks manufactured by National Aperture, Inc. These motor stacks give submicron precision in the placement of optics, but we have some evidence from X-ray holography experiments that they have some positional vibration at the 100 nm level. One of the motor stacks is positioned upstream of the sample, while the other is downstream of the sample. The optics mounts are designed to hold several optical components, and in the case of the downstream motors the mount allows one to reach around and place a component in the beam path upstream of the specimen as well as downstream. This gives us flexibility to change optical components without breaking vacuum.

All stages are driven by DC motors with optical encoders. These motors are controlled by two Galil DMC-2180 motion controllers with ethernet interfaces on a private network. We developed a custom amplifier that provides the necessary current to drive the motors, and routes the drive currents and encoder signals to connectors used by the JEOL

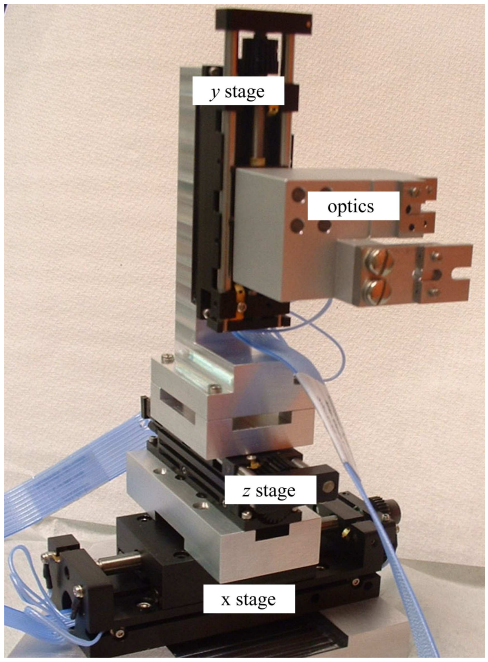


Fig. 5. One of the two $xyz$ motorized translation stage stacks used to hold optics and beam defining apertures. The height of the assembly from the bottom of the $x$ stage to the upper-most protrusion of the $y$ stage is 15 cm.

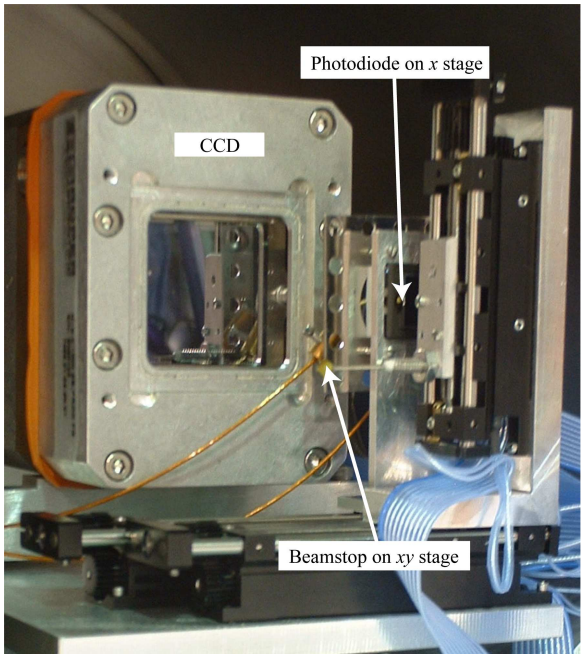


Fig. 6. CCD camera with beamstop and photodiode stages. The beamstop can be moved along the $x$- and $y$-axis, while the photodiode and CCD may be moved along the $x$-axis. The entire unit is mounted on a platform which can be translated from outside along the $z$-axis.

goniometer system, and to vacuum feedthroughs for the two in-vacuum $xyz$ motor stacks.

### 3.3. *Detector system*

The detector is an in-vacuum, backside-illuminated CCD camera from Roper Scientific, Inc. (MTE-2 camera with EEV chip, 1340x1300 pixels with 20 micron pixel size and a claimed readout noise of 4 electrons rms per pixel in its best acquisition mode; see Fig. 6).

The CCD chip is maintained at a temperature of $-45°$ C during normal operation through the use of a Peltier cooling stack, with water flow connections through the vacuum chamber walls to carry off heat from the cooling stack and the camera electronics. With this cooling arrangement, we measured a dark noise of 0.5 to 1.5 electrons per pixel per second. By using thermoelectric rather than liquid nitrogen cooling, the camera system can be warmed up relatively quickly in case the vacuum chamber needs to be vented to atmospheric pressure. The detector system is mounted on an in-vacuum linear bearing assembly so that it can be translated along the beam axis (the $z$ direction) over a range of 17 cm without breaking vacuum. Extension tubes can also be installed to move the CCD farther downstream for selected experiments. The CCD face can be moved as close as about $z = 10$ cm from the specimen, so that it can record information over an angular range of more than 7° on either side of the optical axis (corresponding to diffraction from half-periods of 6.4 nm at 750 eV and 9.2 nm at 520 eV). When moved to 27 cm from the specimen, a Fresnel zone plate with 1 mm focal length can be inserted downstream of the specimen and used to record a coherent brightfield image with an optical magnification of 270 and a real space pixel size of 74 nm. While coherent illumination is not ideal for direct imaging, and the resolution is poor compared to optimized soft X-ray microscopes, this image can still be used to identify and center specimens prior to recording their diffraction patterns. Fig. 7 shows such a recorded image

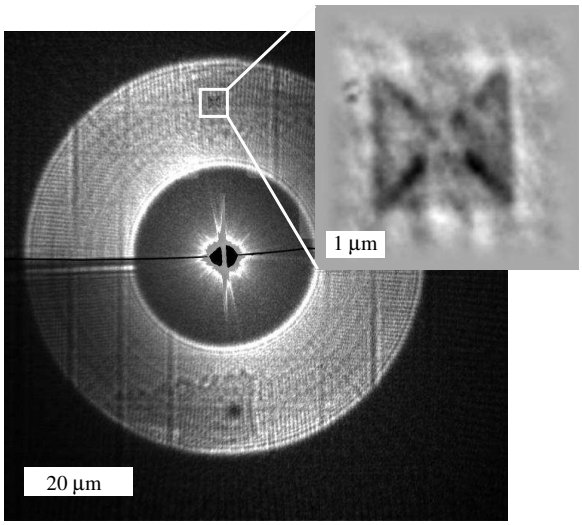


Fig. 7. Real-space image of the pyramid sample recorded in the apparatus using a 80 $\mu$m diameter nickel zone plate with 20 nm outermost zones [20]. The image shows the pyramid in positive first order focus (top) and out of focus from the negative first order of the zone plate. The inset shows a magnified version of the image produced by the positive first-order focus. This inset image is also smoothed at the edges for subsequent image manipulation.

of a specimen fabricated by a Livermore-Arizona-Advanced Light Source collaboraton. It involves a hollow silicon nitride pyramid decorated with 50 nm gold balls [19].

In practice, it is often sufficient to place the coherence-defining pinhole a distance of 25 mm from the sample and use a simple pinhole projection image to accomplish this task (Fig. 8).

The signal at the CCD camera plane includes a very strong undiffracted beam with a width of only a few pixels, and a diffraction signal that declines roughly as the fourth power of diffraction angle [21]. Since the full-well capacity of the CCD is only about 200,000 electrons or (assuming 80 % detective quantum efficiency) about 1217 photons at 750 eV, this means that it is easy to saturate the central pixels of the CCD while attempting to record the weaker but higher resolution signal at higher angles. It is therefore important to use a beamstop of appropriate size to prevent radiation damage to the center CCD pixels and to minimize charge bleeding from saturated pixels to their neighbors. While a variable attenuation beamstop is in the

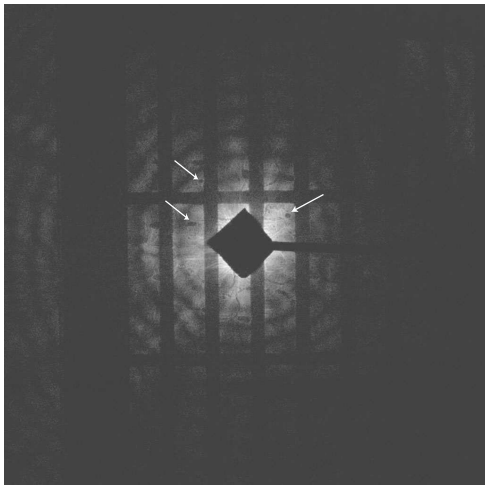

Fig. 8. A simple pinhole projection image can also be used to locate and center suitable specimens. This image shows the slotted copper grid with several yeast cells (indicated by arrows) lying on a carbon support film. This image was taken with a distance of 25 mm between the 4 $\mu$m diameter pinhole and the specimen grid at an energy of 525 eV.

planning stages, at present we use opaque beamstops that are positioned by a $xy$ motor stack in front of the CCD camera. We also have a photodiode for absolute flux measurement located between this beamstop and the CCD. The photodiode can be moved by a motorized translation stage in the $x$ direction.

### 3.4. *Chamber and support system*

The microscope chamber has a number of viewports through which the X-ray beam can be seen on phosphor screens. A swinging, sealable access door (14 cm internal diameter) provides an easy way of reaching into the chamber to switch optical components on the stages. The whole experimental chamber is mounted on a moveable frame, equipped with actuators that allow positioning of the experimental chamber in all directions to a precision of a few tens of micrometers, and allowing for adjustment of tilt. This adjustability has proven useful for both transporting the chamber from the National Synchrotron Light Source at Brookhaven Lab (where it was initially commissioned) to the Advanced Light Source in at Lawrence Berkeley Lab (where it is now operated) and rapid adjustment to follow

changes in beamline optics and alignment.

### 3.5. *Vacuum system*

When working with specimens at liquid nitrogen temperature, low pressures are required to prevent the sample from building up a contamination layer due to condensation of residual gases such as water. At the same time, it is desirable to be able to open the vacuum chamber to exchange optics without the time required for bakeout of an ultra high vacuum system. Our apparatus operates at a pressure of below $10^{-7}$ torr when a room temperature specimen is loaded; this pressure is achieved by using an oil-free pump (Alcatel ACP20) for initial evacuation, and a 60 liter per second turbomolecular pump mounted directly to the experimental chamber through a gate valve with a 6 cm internal diameter (MDC, GV-2500V-P). The chamber has also been designed to accommodate a 150 liter per second ion getter pump through a 10 cm internal diameter gate valve (MDC, GV-4000V-P), with the idea that this pump would be used at the lowest pressures and for minimum vibration. However, the turbo pump has provided sufficient vacuum for our present experiments, so the ion getter pump is not presently mounted.

Two additional features are crucial for operation with frozen hydrated specimens: an airlock and a cold finger. The airlock is pumped with a 100 liters per minute dry scroll pump from Varian, Inc. to minimize exposure of the specimen grid to humid air while it is in its cold metal sleeve. The cold finger has been built into the chamber to minimize contamination buildup. The cold finger involves a copper plate with a surface area of about 220 $cm^2$ which is connected by a copper rod to a 0.2 liter liquid nitrogen reservoir. When the dewar is filled with liquid nitrogen, the base pressure in the experimental chamber falls from below $10^{-7}$ torr to below $10^{-8}$ torr.

A combination of convectron and cold cathode ionization gauges is used to monitor the pressure inside the vacuum chamber and in the airlock region. An interlock (made of programmable logic controllers from Omron, with a color touchscreen user interface) monitors the pressure in these gauges and closes the gate valve to protect the turbomolecular pump in case of accidental venting of the chamber such as by improper sealing of the butterfly valve in the goniometer system. This interlock system also monitors the water cooling flow to the CCD camera; in case of low flow, electrical power will be disconnected from the CCD camera controller.

### 3.6. *Control software*

Manufacturer-supplied programs exist to control individual elements of the diffraction system (the CCD camera, and the controller for the goniometer and optics mount motors). However, since we wish to record exposure sequences through a range of rotations of the specimen, it was our desire to integrate these components into a single user interface with automation capabilities. For this reason, we have developed a client-server software package to control the microscope. This package consists of three elements:

(i) The server program (written in C/C++) talks to the CCD camera controller and motor controllers through manufacturer-supplied drivers and subroutine libraries. The server program also communicates with an EPICS node in the Advanced Light Source control system to obtain up-to-date information on storage ring current and beam availability.

(ii) The client subroutines (written in the IDL programming language from Research Systems, Inc.) send requests to the server and collects responses from it, using standard TCP/IP sockets.

(iii) Various programs make use of the client subroutines to provide the user with a means to control the apparatus and display data. In most cases, a graphical user interface is used to do this in a very interactive fashion. However, a script-based program is also available to instruct the apparatus to carry out a predetermined sequence of operations, and users may write their own programs to call upon the client routines.

This modular software approach has allowed different people to be responsible for specific parts of the overall software package, with coordination provided by the Concurrent Version System software package (`http://www.cvshome.org`). The use of client-server sockets makes it possible to operate the apparatus from remote locations with the users' machine managing the graphical user interface or GUI. The GUI program can also be run in a mode where it does not connect to the hardware (a mode used primarily for image evaluation). The entire control system runs on a PC workstation running the Linux operating system.

## 4. Experimental diffraction data

The microscope system is currently mounted on beamline 9.0.1 [18] at the Advanced Light Source at Lawrence Berkeley Laboratory. It is used by the Stony Brook group primarily for imaging biological specimens [22] (??? update citation details once we know from the reviewers), and by a group involving Lawrence Livermore National Lab, Arizona State University, and the Advanced Light Source for imaging manufactured and materials specimens [19] (??? update citation details once we know more from the reviewers). Fig. 9 shows an example data set acquired by the Livermore-Arizona-Advanced Light Source team using the diffraction microscope system.

This example dataset was generated by combining several diffraction patterns with exposure times of 0.5 s and 100 s. In this particular image, the Fourier transform of the real-space image was used to fill in the region behind the beam stop in the diffraction pattern recording, although in practice one can also reconstruct the image from the diffraction data alone [6]. Successful reconstructions of experimental data will be published elsewhere [22], [19].

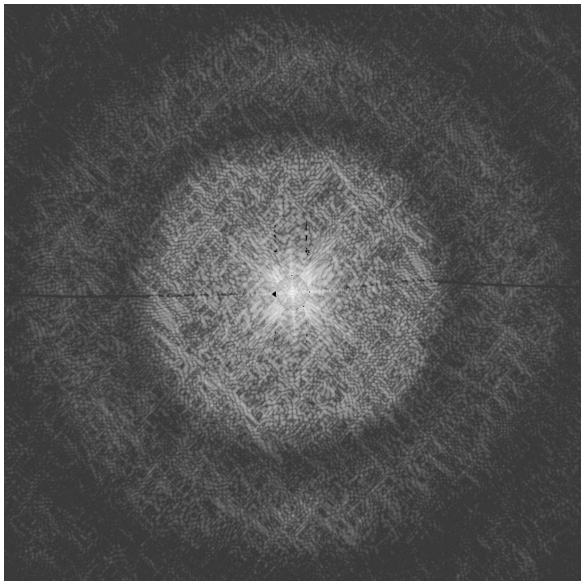

Fig. 9. Example data recorded with the diffraction microscope system. This example shows the combined diffraction pattern of the pyramid sample on a logarithmic scale as recorded by the Livermore-Arizona-Advanced Light Source team. Several diffraction patterns with various exposure times were added up after a threshold was applied and the intensity was normalized by the exposure time. The central region was filled in with the Fourier transform of the real-space image shown in Fig. 7.

## 5. Conclusions

We have constructed and commissioned an X-ray diffraction microscope system that allows recording of real-space images together with diffraction data. The microscope control system allows for automated collection of single-axis tilt sequences to make 3D imaging feasible. Frozen hydrated specimens can be prepared, loaded, and maintained at liquid nitrogen tempertures according to standard electron microscopy protocols; this is crucial for obtaining the maximum possible information from biological specimens. Present experiments are aimed at exploring the maximum spatial resolution that can be obtained with the limitations of radition damage, and at recording 2D and 3D diffraction data from specimens of increasing complexity.

## Acknowledgements

We thank Michael Feser (then of Stony Brook), Sue Wirick of Stony Brook, Barrett Clay of the

NSLS, and the ALS staff for much help with the project. This research was supported by the NSF under grant DBI-9986819 and NIH under grant PHS 1R01 GM648460. The Advanced Light Source is supported by the Director, Office of Science, Office of Basic Energy Sciences, Materials Sciences Division, of the U.S. Department of Energy under Contract No. DE-AC03-76SF00098 at Lawrence Berkeley National Laboratory. The National Synchrotron Light Source is supported by the U.S. Department of Energy, Division of Materials Sciences and Division of Chemical Sciences under contract No. DE-AC02-98CH10886.

## References

[1] C. Jacobsen, J. Kirz, S. Williams, Resolution in soft x-ray microscopes, Ultramicroscopy 47 (1992) 55–79.

[2] D. Sayre, Some implications of a theorem due to Shannon, Acta Crystallographica 5 (1952) 843.

[3] D. Sayre, Prospects for long-wavelength x-ray microscopy and diffraction, in: M. Schlenker, M. Fink, J. Goedgebuer, C. Malgrange, J. Viénot, R. Wade (Eds.), Imaging Processes and Coherence in Physics, Vol. 112 of Lecture Notes in Physics, Springer-Verlag, 1980, pp. 229–235.

[4] J. Miao, P. Charalambous, J. Kirz, D. Sayre, An extension of the methods of x-ray crystallography to allow imaging of micron-size non-crystalline specimens, Nature 400 (1999) 342–344.

[5] I. Robinson, I. Vartanyants, G. Williams, M. Pfeifer, J. Pitney, Reconstruction of the shapes of gold nanocrystals using coherent x-ray diffraction, Physical Review Letters 8719 (19) (2001) 195505.

[6] S. Marchesini, H. He, H. Chapman, S. Hau-Riege, A. Noy, M. Howells, U. Weierstall, J. Spence, X-ray image reconstruction from a diffraction pattern alone, Physical Review B 68 (14) (2003) 140101.

[7] R. W. Gerchberg, W. O. Saxton, A practical algorithm for the determination of phase from image and diffraction plane pictures, Optik 35 (2) (1972) 237–246.

[8] J. Fienup, Phase retrieval algorithms: a comparison, Applied Optics 21 (5) (1982) 2758–2769.

[9] V. Elser, Phase retrieval by iterated projections, Journal of the Optical Society of America A 20 (1) (2003) 40–55.

[10] R. Glaeser, K. Taylor, Radiation damage relative to transmission electron microscopy of biological specimens at low temperature: a review, Journal of Microscopy 112 (1978) 127–138.

[11] Y. Wang, C. Jacobsen, J. Maser, A. Osanna, Soft x-ray microscopy with a cryo STXM: II. Tomography, Journal of Microscopy 197 (1) (2000) 80–93.

[12] D. Weiß, G. Schneider, B. Niemann, P. Guttmann, D. Rudolph, G. Schmahl, Computed tomography of cryogenic biological specimens based on x-ray microscopic images, Ultramicroscopy 84 (2000) 185–197.

[13] C. Larabell, M. Le Gros, X-ray tomography generates 3-D reconstructions of the yeast, *saccharomyces cerevisiae*, at 60-nm resolution, Molecular Biology of the Cell 15 (2004) 957–962.

[14] J. Miao, T. Ishikawa, B. Johnson, E. Anderson, B. Lai, K. Hodgson, High resolution 3D x-ray diffraction microscopy, Physical Review Letters 89 (8) (2002) 088303.

[15] J. Miao, D. Sayre, H. Chapman, Phase retrieval from the magnitude of the Fourier transforms of non-periodic objects, Journal of the Optical Society of America A 15 (6) (1998) 1662–1669.

[16] T. Beetz, Soft x-ray diffraction imaging with and without lenses and radition damage sudies, Ph.D. thesis, Department of Physics & Astronomy, Stony Brook University (2004).

[17] J. Spence, U. Weierstall, M. Howells, Coherence and sampling requirements for diffractive imaging, Ultramicroscopy 101 (2004) 149–152.

[18] M. Howells, P. Charalambous, H. He, S. Marchesini, J. Spence, An off-axis zone-plate monochromator for high-power undulator radiation, in: D. Mancini (Ed.), Design and Microfabrication of Novel X-ray Optics, Vol. 4783, SPIE, 2002, pp. 65–73.

[19] H. Chapman, The title, in preperation.

[20] S. Spector, C. Jacobsen, D. Tennant, Process optimization for production of sub-20 nm soft x-ray zone plates, Journal of Vacuum Science and Technology B 15 (6) (1997) 2872–2876.

[21] M. Howells, T. Beetz, H. Chapman, C. Cui, J. Holton, C. Jacobsen, J. Kirz, E. Lima, S. Marchesini, H. Miao, D. Sayre, D. Shapiro, J. Spence, An assessment of the resolution due to radiation-damage in x-ray diffraction microscopy, Journal of Electron Spectroscopy and Related Phenomena in press.

[22] D. Shapiro, P. Thibault, T. Beetz, V. Elser, M. Howells, C. Jacobsen, J. Kirz, E. Lima, H. Miao, D. Sayre, Biological microscopy by soft x-ray diffraction imaging, in preparation.